IIETA International Information and Engineering Technology Association
Advancing the World of Information and Engineering

Revue des Composites et des Matériaux Avancés-Journal of Composite and Advanced Materials
Vol. 35, No. 1, February, 2025, pp. 117-126
Journal homepage: http://iieta.org/journals/rcma

Effects of Flowing Water Cooling on the Quenching Process of AISI 1045 Steel: Influence on Tensile Strength, Hardness, and Microstructure

Enos Tambing[1], Agustinus[1], Thomas Pagasis[1], Obet Takke Ranteallo[1], David Mangallo[1], Joni[2*]

[1] Department of Mechanical Engineering, Cenderawasih University, Jayapura 99351, Indonesia
[2] Renewable Energy Engineering, Graduate School of Cenderawasih University, Jayapura 99351, Indonesia

Corresponding Author Email: joni@ftuncen.ac.id

https://doi.org/10.18280/rcma.350114

Received: 6 January 2025
Revised: 20 January 2025
Accepted: 11 February 2025
Available online: 28 February 2025

Keywords:
AISI 1045 steel, cooling water flow, cooling rate effects, martensitic transformation, micro structure, mechanical property enhancement, quenching

ABSTRACT

This study investigated the effects of water quenching on the mechanical properties and microstructure of AISI 1045 steel. The aim was to optimize martensite formation through the development of a water flow cooling system. An experimental setup was designed using a 100 L drum as the cooling vessel, equipped with a pump and valve system to maintain a constant water flow rate of 15 L/min. The test specimens comprised 15 low-carbon steel bars, each measuring 20 mm × 185 mm. The specimens were heated in a furnace with a maximum capacity of 1200℃, with six bars heated to 820℃ and the other six to 900℃. Tensile and hardness tests, along with microstructural analyses, were conducted to evaluate the effects of quenching under these conditions. The results demonstrated that water flow quenching significantly enhanced martensite formation, improving mechanical properties compared to conventional quenching methods. Specifically, quenching at 820℃ led to a tensile strength increase of approximately 20.16% and a hardness improvement of 61.73%. Microstructural analysis revealed that specimens quenched with water flow exhibited a more uniform martensitic structure. These findings confirm that employing a circulating water flow system during quenching enhances both mechanical properties and microstructural uniformity. The observed improvements in AISI 1045 steel's performance underscore the potential of this method for industrial applications requiring superior strength and hardness. This study provides a foundation for further research into optimizing the quenching process for low-carbon steels.

1. INTRODUCTION

Material characteristics are paramount in engineering as they directly affect the efficacy, longevity, and safety of the ultimate product. Among the diverse materials that are frequently employed, AISI 1045 steel is distinguished in numerous engineering applications due to its exceptional mechanical attributes. Numerous investigations have also underscored how varying cooling velocities and media, such as aqueous solutions, lubricants, and polymers, impact the quenching process and modulate the resultant mechanical properties and microstructure of this steel. This classification of steel, recognized as medium carbon steel with a carbon content ranging between 0.43% and 0.50%, demonstrates enhanced strength and hardness relative to low carbon alternatives [1, 2]. These traits render it an optimal selection for applications necessitating wear resistance and strength, such as automotive components—for instance, axles, bolts, and connecting rods [2, 3]. Within engineering contexts, AISI 1045 steel is recognized for its capacity to endure substantial loads while preserving its structural integrity. This renders it preferable in sectors that require dependable materials that perform admirably under duress [4]. Moreover, the mechanical characteristics of this steel can be augmented through thermal processing techniques, encompassing quenching and tempering methods, which enhance its hardness and wear resistance [1, 5]. Research has indicated that heat treatment can profoundly alter the mechanical properties of AISI 1045, prolonging its operational lifespan through enhanced fatigue resistance [6, 7].

Quenching is a swift cooling method employed post-austenitization of steel. The selection of quenching medium, including water, oil, or polymer solution, critically affects the resultant hardness of the steel. For example, Vieira et al. found that AISI 1045 steel quenched with polymer solutions at various concentrations showed variations in hardness, where higher concentrations resulted in better hardness due to more controlled cooling rates [7]. Similarly, Nasution's research showed that the use of oil or water in the quenching process can increase the hardness and strength of the steel, which is very important for applications that require high wear resistance [1].

Induction hardening enhances the properties of AISI 1045. This method utilizes electromagnetic induction heating

followed by rapid cooling. As reported by Gao et al. [8], this technique can elevate surface hardness to approximately 700 HV. The hardening depth can be manipulated through variations in heating duration and cooling rates, enabling tailored mechanical properties for specific applications [9].

Tempering is conducted post-quenching to alleviate internal stresses and minimize brittleness. The parameters of tempering, specifically temperature and duration, are critical in defining the properties of AISI 1045. Research indicates that tempering temperature variations influence hardness and toughness, with optimal conditions facilitating a compromise between the two [5, 7]. The synergistic process of quenching and tempering is essential in developing the requisite microstructure for targeted strength and ductility in engineering applications.

Despite extensive studies on various quenching methods for steel, the specific effects of flowing water quenching on AISI 1045 steel remain underexplored. Most studies have focused more on conventional quenching methods, such as the use of oil or polymers, without considering the role of flowing water which can actually affect the cooling rate and the resulting microstructural changes [10, 11]. The existing literature generally provides a qualitative assessment of how different cooling media impact the mechanical properties of steel, but in-depth quantitative studies are still needed to understand how the flowing water cooling rate affects the tensile strength, hardness, and microstructural changes of AISI 1045 steel [1, 12]. On the other hand, the relationship between the cooling rate and the microstructural changes that occur, such as the formation of martensite or bainite in AISI 1045 steel, has not been adequately documented in the context of flowing water cooling. Existing studies [13, 14] have focused more on microstructural changes under general cooling conditions, but studies that specifically focus on flowing water cooling are still limited. Moreover, the effects of variations in water flow rate and temperature on the cooling effectiveness and final properties of AISI 1045 steel remain inadequately studied. Research in this area could yield valuable insights for optimizing cooling processes to meet industrial requirements [15]. To address this, the objectives of this study are to investigate the effects of flowing water quenching on the tensile strength, hardness, and microstructural changes in AISI 1045 steel, providing a deeper understanding of the cooling rate's influence on these critical properties. Consequently, additional investigation on the cooling utilizing flowing water is imperative, particularly to comprehend its implications on mechanical characteristics, such as tensile strength and hardness, in addition to alterations in the microstructure of AISI 1045 steel.

2. MATERIALS AND METHODS

2.1 Materials

The investigation focused on AISI 1045 steel, recognized for its beneficial mechanical attributes and machinability. Spectrometric analysis revealed a composition of 98.51% Fe. The carbon content was determined to be 0.47%. Manganese was measured at 0.511%. Phosphorus was identified at 0.028%. Sulfur was quantified at 0.009%. Silicon content was evaluated at 0.089%. The carbon percentage of 0.47% enhances hardness and strength after heat treatment, while 0.511% manganese improves hardenability and toughness. The phosphorus and sulfur levels, at 0.028% and 0.009%, respectively, enhance machinability and reduce brittleness. Silicon, at 0.089%, is crucial for augmenting tensile strength and resistance to deformation in the steel (refer to Figure 1).

The steel is in the form of a cylindrical bar with a diameter of 20 mm and a length of 185 mm. A total of 15 specimens were prepared, consisting of 3 untreated specimens, 6 specimens subjected to heat treatment at a temperature of 820°C, and 6 specimens subjected to heat treatment at a temperature of 900°C. Each bar was cut and processed into standard specimens for tensile, hardness, and microstructure analysis, guided by the ASTM E8M and ASTM E12 standards. These specimens were prepared with attention to the uniformity of dimensions and composition to minimize variability and ensure consistent results during the cooling process and subsequent characterization.

Figure 1. AISI 1045 steel specimen

2.2 Experimental setup

The cooling apparatus was constructed utilizing a repurposed 200-liter drum, bisected to create the primary cooling mechanism (Figure 2). The drum's base was equipped with 1-inch water inlet and outlet conduits for the circulation of cooling water. A 1-inch ball valve was incorporated at the outlet to manage water flow and ensure regulated circulation throughout the cooling operation. The water supply system employed a Sanyo P-H137AC pump capable of delivering a maximum of 30 liters per minute to sustain a steady water flow. Two 200-liter drums were interconnected via 1-inch pipes at both the upper and lower sections, functioning as supply reservoirs to guarantee adequate water volume for continuous cooling.

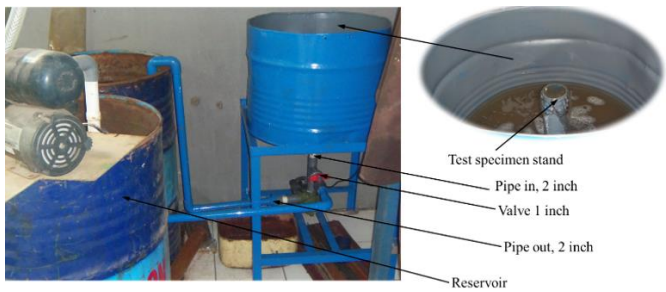

Figure 2. Schematic of the cooling water installation system

The control parameters were scrupulously calibrated to augment the effectiveness of the cooling process. The flow rate of the cooling water was methodically regulated via an integration of a ball valve and a pump system to guarantee homogenous circulation of the fluid. Moreover, the temperature of the cooling water was rigorously tracked and

perpetually maintained at 24°C to promote optimal thermal transfer throughout the cooling operation. Meanwhile, the final cooling temperature of the AISI 1045 steel specimen was set at 50°C before being removed from the cooling water medium.

The heat treatment procedure begins by heating AISI 1045 steel material measuring 20 mm × 185 mm in a furnace (Figure 3) at the specified temperatures of 820°C and 900°C. The holding time during the heating process in the furnace is 60 minutes; this aims to form a homogeneous austenite microstructure. After that, the specimen is cooled rapidly to a temperature of 50°C. Cooling is carried out under two conditions: flowing water (circulating) and non-flowing water (without circulation).

Figure 3. Furnace with 2 kW capacity

The specimens were coded according to the type of treatment received. Specifically, Q_0 refers to normal specimens (without treatment), Q_1 is the code for specimens cooled without circulation flow, and Q_2 is the code for specimens cooled with circulation flow. Cooling without circulation was carried out in a water pool with a capacity of 40 L, while cooling with circulation was conducted in flowing water conditions at a speed of 15 L/min, which was regulated by a valve, to cool the specimens until their temperature reached 50°C. Normal and heat-treated specimens that had cooled were then prepared for tensile, hardness, and microstructure testing purposes.

2.3 Testing and characterization of specimens

Testing and characterization of AISI 1045 steel assess its mechanical properties and microstructure post-quenching. Tensile strength is quantified per ASTM E8M standards via a universal testing machine to evaluate load resistance. Hardness is evaluated using the Rockwell (HRC) method in accordance with ASTM E12 standards to determine surface strength and deformation resistance. Microstructural examination employs a metallographic microscope to analyze grain morphology and phase transformations, including martensite and retained austenite, induced by quenching.

2.3.1 Tensile strength

Tensile strength tests were conducted three times each for untreated specimens, flowing water-cooled specimens, and non-flowing water-cooled specimens. These tests allow for a comprehensive analysis of the changes in material characteristics due to different heat treatments and cooling conditions. The tensile specimens were prepared per ASTM E8M standards, as depicted in Figure 4, and their tensile properties were assessed using a SHIMADZU AGX-V2 Series universal tensile tester with a 1000 kN capacity and 10 kHz data acquisition rate; fifteen samples were tested, yielding three data sets each, which were averaged for conclusive analysis.

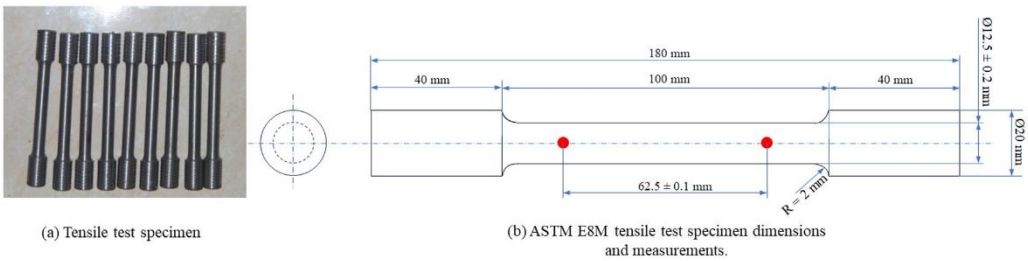

Figure 4. Schematic diagram of a tensile test specimen

The dimensions of the specimen (initial length, initial gauge length, initial diameter, and initial cross-sectional area) were measured by calculating the average of three measurements. Before mounting the specimen on the tensile testing machine, grips were created at the flat ends to prevent slippage during testing. One specimen was mounted onto the machine holder, and the loading scale was set on the machine. The millimeter block and marker were attached to the testing machine, which was then activated, and the load was applied to the specimen. The load values at yield, maximum load, and fracture were observed and recorded with the assistance of the machine operator. The marker plotted the load-elongation curve on the millimeter block in accordance with the testing conditions and the specimen. After fracture, the specimen was removed from the machine holder, and the millimeter block sheet was detached from the testing machine. The millimeter block was labeled to avoid confusion with subsequent test results. The fractured specimen was then manually reassembled, measured, and the post-fracture dimensions (final length, final gauge length, final diameter) were recorded. These steps were repeated for the next specimen.

2.3.2 Hardness test

Surface hardness testing of each specimen, both with and without cooling treatment, was carried out following the ASTM E12 standard at a room temperature of 29°C. Hardness was assessed using the NR3D - Rockwell principle bench hardness tester (Figure 5(a)), with an HRC scale and a conical diamond indenter. The specimen's surface was cleaned and placed on the machine's circular baseplate. The indenter was mounted on the indenter holder, and the load was applied according to the standard of 150 kgf. The baseplate was raised by rotating the handwheel until the small-scale indicator showed the number 3, indicating the initial load of 10 kgf. The

side handle was gently touched to initiate movement, starting the main loading and indentation process. The movement of the side handle was allowed to occur naturally until it stopped, after which it was held for 10 seconds before returning to its starting position. The circular baseplate was then lowered by rotating the handwheel. The specimen was repositioned such that the next indentation was placed approximately 1.5 times the length of the diameter or longest diagonal of the previous indentation. These steps were repeated for additional indentations at different positions and specimens. The hardness value of the indentation was recorded from the machine's main scale.

Each sample was measured sequentially from the edge to the center (Figure 5(b)) at three points: point 1 (2 mm), point 2 (5 mm), and point 3 (9 mm). The measurement position starts at point a, which is located 5 mm from the previously cut base end, and the surface was cleaned using 200-grit sandpaper. This process was also applied to points b, c, and d, which are located 10 mm, 20 mm, and 30 mm from point a, respectively.

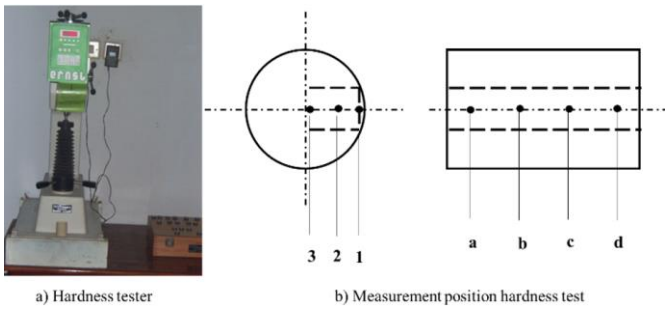

Figure 5. Hardness testing equipment and pressure application points in accordance with ASTM E18 standards

2.3.3 Microstructure

To investigate and analyze the microstructural characteristics of the specimens, a Gonoava GA-2401-A microscope (Figure 6), equipped with a magnification capability of 100X to 1250X, was employed. The initial phase involved the removal of residual contaminants from each specimen's surface, followed by a polishing procedure aimed at enhancing the quality of the results. Subsequently, the specimens underwent a chemical treatment with a mixture of alcohol and 2.5% nitric acid for various exposure durations. This step is critical due to the differing microstructural evolutions experienced by each specimen.

Figure 6. Gonoava GA-2401-A microscope

This microanalytical approach enabled the assessment of grain dimensions and morphology, phase arrangement, and alloy constituents, thereby elucidating the structural characteristics after the various treatments [16]. Chemical etching with the alcohol and nitric acid mixture revealed one specific type of microstructure in the steel, identified as ferrite. All types of steels with a carbon content below 0.85% C that undergo annealing processes produce two distinct phases: pearlite and ferrite. Ferrite has a carbon concentration of 0.008% C and remains unaffected by the reagent, whereas pearlite contains a carbon percentage of 0.85% C and undergoes surface degradation upon exposure to the alcohol and nitric acid mixture. Consequently, the ferrite surface appears planar, and the reflected light is directed into the microscope chamber, creating bright areas observable in the micrograph. In contrast, the surface of pearlite crystals is irregular, causing a heterogeneous light reflection that makes it appear dark. Furthermore, crusts form at the boundaries of the ferrite grains as a consequence of the Nital treatment, resulting in the edges of the crystals appearing dark in the micrograph.

3. RESULTS AND DISCUSSION

This analysis explores how quenching, whether performed with or without circulation, influences the mechanical characteristics and microstructure of AISI 1045 steel after undergoing heat treatment. Prior to quenching, various heat treatment temperatures were applied. Analysis reveals that both hardness and mechanical strength diminish as heat treatment temperature increases, specifically at 820°C and 900°C. This finding supports the Fe-C phase diagram theory, indicating that the ideal hardening temperature for AISI 1045, with approximately 0.47% carbon, lies between 820°C and 900°C.

3.1 Cooling rate

The heating, holding, and cooling processes of AISI steels heated at 820°C and 900°C are illustrated in Figure 7. During the heating phase, the steels reached their target temperatures 820°C for samples 820-Q1 and 820-Q_2, and 900°C for samples 900-Q_1 and 900-Q_2—within approximately 400 to 484 seconds, highlighting the rapid heating process. Once the respective temperatures were attained, the samples were held at a constant temperature for 3600 seconds (1 hour), providing sufficient time for microstructural transformations, such as austenitization, which is critical for enhancing steel properties like strength and ductility [17].

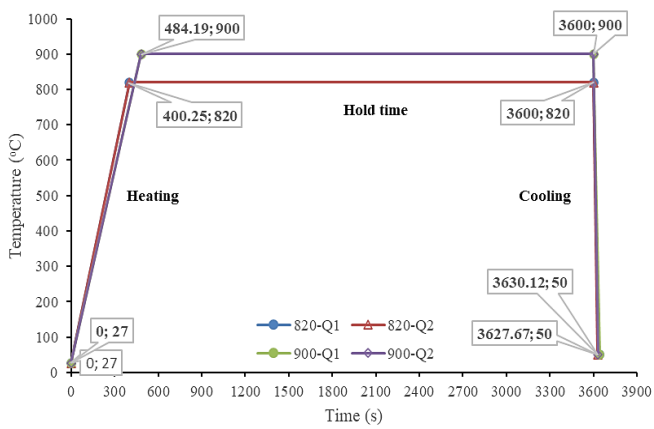

Figure 7. Heating and cooling times

The holding period facilitates microstructural homogenization, minimizes temperature gradients, and promotes phase stability. Notably, the higher temperature of 900°C in samples 900-Q_1 and 900-Q_2 may induce grain growth due to prolonged exposure to elevated temperatures. In contrast, the 820°C treatment (820-Q_1 and 820-Q_2) likely promotes the formation of finer grains, which typically enhances mechanical properties.

During the cooling phase, the steel temperature rapidly decreased to 50°C within approximately 3,600 to 3,630 seconds, confirming a controlled cooling process. The cooling rate is a critical factor in determining the final mechanical properties of steel. Rapid cooling can suppress grain growth and preserve beneficial microstructures, such as fine martensite or bainite, depending on the carbon content of the alloy [18]. Comparatively, cooling from 900°C can result in a coarser microstructure, as the grains tend to grow during the holding phase. This observation aligns with the lower tensile strength values recorded for samples 900-Q_1 and 900-Q_2 in the previous analysis. Conversely, controlled cooling from 820°C likely maintains finer grains and a balanced phase composition, thereby optimizing both strength and ductility.

This analysis confirms that heating and holding temperatures, in conjunction with cooling rates, significantly impact the microstructural evolution and mechanical behavior of AISI 1045 steels [19]. The cooling rate also plays a crucial role in determining the relative proportions of ferrite and pearlite in low-carbon steels by regulating the diffusion rate during austenite decomposition. At slower cooling rates, the system allows sufficient time for carbon atoms to diffuse out of the austenite phase, favoring the formation of ferrite, which is low in carbon. Ferrite nucleates at grain boundaries and grows into austenite grains, while the remaining carbon-enriched austenite transforms into pearlite. Consequently, the steel exhibits a higher proportion of ferrite, which imparts ductility and toughness but reduces overall strength and hardness.

Increasing the cooling rate limits carbon diffusion, leading to the dominance of pearlite formation due to the lamellar structure of ferrite and cementite. Higher cooling rates suppress ferrite formation, resulting in a greater proportion of pearlite, which enhances strength and wear resistance but may sacrifice some ductility. At faster cooling rates, the formation of ferrite and pearlite can be bypassed altogether, allowing for the development of other microstructures, such as bainite or martensite. Following heat treatment and subsequent water cooling, varying cooling rates were achieved for each specimen undergoing different treatments, as shown in Figure 8. The cooling time was recorded when each specimen reached a final temperature of 50°C.

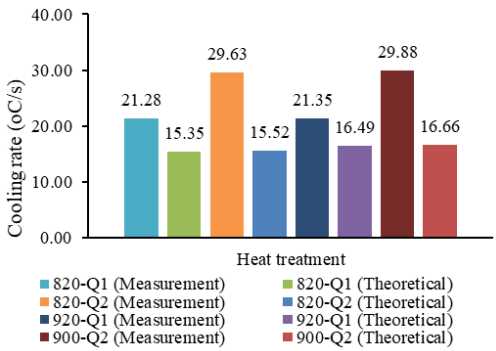

Figure 8. Comparison of cooling rates

The cooling time of AISI 1045 steel during isothermal transformation significantly affects the formation of various microstructural phases, including pearlite, bainite, and martensite. Each cooling duration influences the kinetics of the phase transformation, which is critical for optimizing material properties. Shorter cooling times, such as 23.79 seconds, tend to favor the formation of martensite due to rapid cooling, which suppresses the formation of other phases such as pearlite and bainite. This occurs because austenite does not have enough time to decompose into these phases before transforming into martensite, which is a diffusion less transformation [11, 20]. In contrast, longer cooling times, such as 42.15 seconds, allow for a more extensive diffusion process, favoring the development of bainite and pearlite. Bainite, in particular, forms at lower temperatures and requires a slower cooling rate to develop its characteristic microstructure [7, 20].

Different cooling rates result in different microstructures; for example, cooling times of 34.78 seconds and 38.54 seconds can produce a mixed microstructure of bainite and pearlite, depending on the specific temperature range and isothermal holding rate [10, 21] Additionally, the transformation kinetics-which determine the rate of phase formation-are influenced by these cooling times. Slower cooling rates enhance phase nucleation and growth, allowing for finer microstructures [22, 23].

3.2 Tensile testing results

Isothermal transformation has a significant impact on the mechanical properties of AISI 1045 steel through the formation of microstructures such as bainite and martensite [24]. The carbon content in the initial composition of AISI 1045 steel influences its response to heat treatment and the resulting microstructures. In the isothermal transformation process, heating and cooling parameters are critical in determining the final outcome [25]. Austempering, an isothermal transformation of austenite into bainite, is known to enhance the strength and toughness of AISI 1045 steel. The specific temperature and duration of isothermal holding directly affect the stability of the resulting microstructures, where longer holding times produce more stable microstructures, while shorter durations result in metastable forms [26]. Additionally, the cooling rate during heat treatment plays a vital role: rapid cooling induces martensitic transformation, increasing hardness and strength due to the non-diffusive nature of this phase transformation [27]. In contrast, slower cooling promotes bainite formation, which offers an optimal combination of strength and toughness [21, 28].

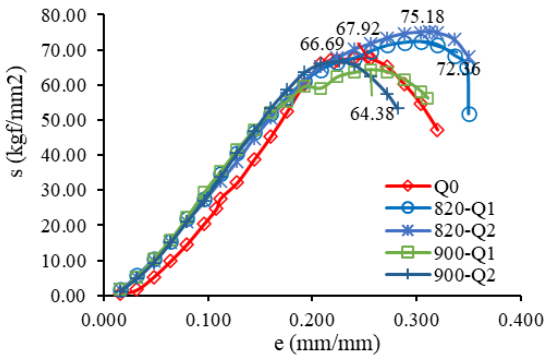

Figure 9. The graph of the relationship between tensile stress and strain

Post-heat treatment cooling methods also significantly influence the tensile properties of the material. Cooling with flowing water (Q_2) results in superior mechanical properties compared to stagnant water cooling (Q_1), attributed to its faster cooling rate and greater ability to refine the microstructure. Figure 9 illustrates the relationship between tensile stress and strain for specimens heated at 820°C and 900°C and subjected to water cooling. The control specimen (Q_0), which was not heat-treated, exhibits the lowest peak tensile strength of 66.69 kgf/mm² and a relatively shorter strain at failure. In contrast, specimens subjected to heat treatment with stagnant water cooling (Q_1) or flowing water cooling (Q_2) show significant improvements in tensile strength and strain. Notably, specimens heated at 900°C and cooled with flowing water (900-Q_2) achieve the highest tensile strength of 75.18 kgf/mm² and the longest strain at failure, reflecting enhanced ductility and strength due to rapid cooling and more pronounced microstructural transformation.

Figures 10 and 11 illustrate the relationship between tensile strength (σ) and strain (ε) for AISI 1045 steel heat-treated at 820°C and 900°C, followed by cooling to 50°C. The Q_0 condition (without heating) exhibits the lowest tensile strength, peaking at approximately 67.92 kgf/mm², indicating the limitations of the material in its untreated state. In contrast, the 820°C treatment (820-Q_1 and 820-Q_2) shows a significant increase in tensile strength, with 820-Q_2 reaching a maximum of 75.18 kgf/mm². This increase can be attributed to microstructural refinement, as heating at 820°C promotes grain boundary strengthening and partial phase transformation, both of which are known to enhance the strength of the material [17]. On the other hand, the 900°C treatment (900-Q_1 and 900-Q_2) exhibited a decrease in tensile strength, with values of approximately 64.38 kgf/mm² and 66.69 kgf/mm², respectively. The reduction in strength at 900°C may be attributed to grain coarsening or carbide dissolution at elevated temperatures, which weakens the load-bearing capacity of the material [18].

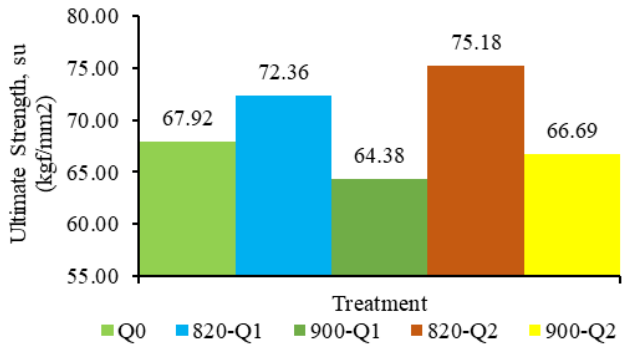

Figure 10. Comparison of tensile strength of AISI 1045 steel under various heat treatment conditions

The strain behavior further highlights the impact of heat treatment on mechanical performance. The Q_0 condition, without heat treatment, shows limited strain capacity, reflecting its relatively low ductility. In comparison, the 820°C treatment not only achieves higher tensile strength but also demonstrates an increase in strain to failure, indicating an optimal balance between strength and ductility. This balance is crucial for practical applications, as it ensures structural reliability under varying loads [19]. For the 900°C condition, although the tensile strength decreases slightly, the ductility remains high, particularly in the 900-Q_1 condition, due to the recovery mechanism that occurs at elevated temperatures. This finding aligns with previous studies on AISI 1045 steel, which identified a heating temperature around 820°C as the optimal temperature for enhancing mechanical properties through grain refinement and phase transformation [17, 18].

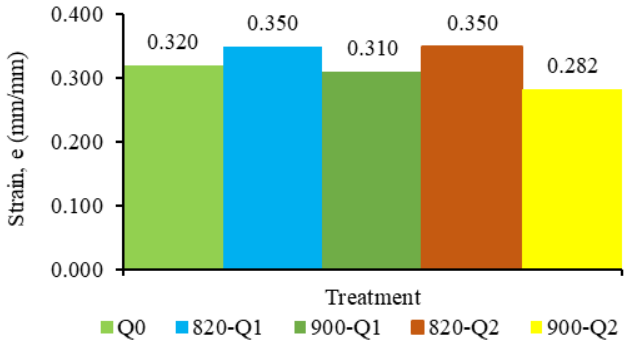

Figure 11. Comparison of strain behavior in AISI 1045 steel under various heat treatment conditions

3.3 Hardness testing results

The surface hardness of AISI 1045 steel is greatly influenced by the cooling medium used during the heat treatment process. When AISI 1045 steel is heated to austenitization temperatures of 820°C and 900°C, the resulting microstructure and hardness depend on the cooling rate achieved by the cooling medium [29, 30]. In untreated AISI 1045 steel specimens, the average hardness value is 13.7 HRC. The data indicate that, for the 820°C heat treatment, the average hardness values are 32.0 HRC for the Q_1 process and 35.8 HRC for the Q_2 process. The increase in hardness from Q_0 to Q_1 was 164.4%, while Q_2 increased by 23.7% compared to Q_1. At 900°C heat treatment, the average hardness values are 28.0 HRC for Q1 and 32.0 HRC for Q_2 (see Figure 12). This increase can be attributed to microstructural transformations, such as the formation of fine-grained martensite or bainitic phases, which are known to enhance hardness due to higher dislocation density and finer grain structure [17]. In particular, Q_2 at 820°C reached a maximum hardness value of 37.85 HRC, likely due to the optimized combination of temperature and holding time that promoted effective phase transformation.

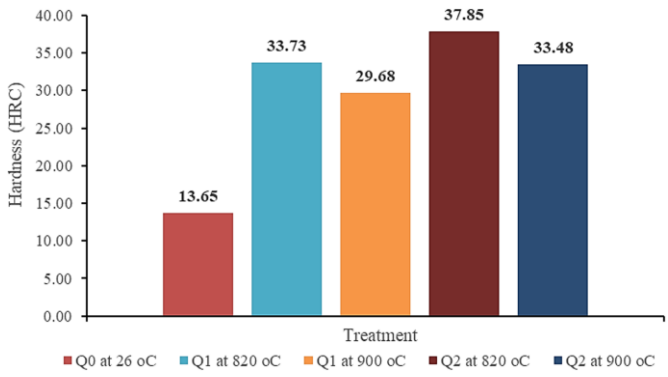

Figure 12. Comparison of hardness values of AISI 1045 Steel under different heat treatment conditions

Quenching in aqueous solutions typically yields the most elevated cooling velocity and the development of a martensitic microstructure, which imparts optimal surface hardness.

Accelerated quenching in aqueous solutions inhibits the development of more ductile microstructures such as pearlite and bainite, resulting in a predominantly martensitic configuration characterized by elevated hardness [29, 30]. In comparison, heating the steel to 900℃ results in slightly lower hardness values, with Q1 and Q2 showing 29.68 HRC and 33.48 HRC, respectively. While the steel still hardens compared to the untreated condition, the reduced hardness at 900℃ can be attributed to grain coarsening, which occurs at high temperatures and leads to a reduction in the number of grain boundaries, thereby reducing hardness [18]. These results confirm that heat treatment at 820℃ provides superior hardness due to a refined microstructure, whereas excessive heating at 900℃ compromises this increase due to grain growth. This analysis aligns with findings that emphasize the important role of heat treatment temperature in achieving desired mechanical properties [31].

3.4 Microstructure

Transformations in AISI 1045 steel during cooling are influenced by its chemical composition and cooling rate. The steel, composed of 98.51% Fe, 0.47% C, 0.511% Mn, 0.028% P, 0.009% S, and 0.089% Si, when heated to 820℃ and cooled for 38.54 seconds, produces a balanced mixture (50% each) of pearlite and bainite, suitable for applications requiring moderate toughness and strength. A faster cooling time of 27.67 seconds allows bainite and martensite to form (20-30% martensite), increasing the hardness. At 900℃, a slower cooling time of 42.15 seconds leads to a predominantly bainitic microstructure (70-80%) with some pearlite (20-30%). During 30.12 seconds, rapid cooling passes through the pearlite and bainite regions, forming a mixture of ~50-60% bainite and ~40-50% martensite, offering the highest hardness. This result aligns with studies on microstructural transitions of steel using TTT and CCT diagrams, which emphasize the role of cooling rate and austenitization temperature in phase formation [17, 32].

Figure 13 illustrates the microstructural characteristics of an untreated AISI 1045 steel specimen. The microstructure of the raw material specimen is what is present at room temperature. From the microstructure photo, the grain boundaries between the phases are still very clear. Ferrite (α) is indicated by light-colored grains, while pearlite is indicated by dark-colored grains. Pearlite consists of iron carbide (Fe_3C) and α (ferrite), where the amount of ferrite in the raw material is greater than that of pearlite. The microstructure of the examined AISI 1045 steel specimen devoid of thermal treatment is constituted of 88% pearlite (α + Fe_3C) and 12% allotriomorphic ferrite (α), establishing the primordial austenite grains.

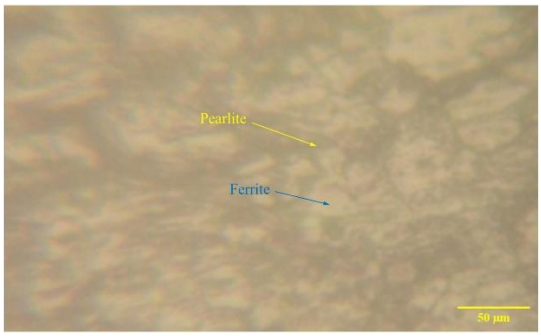

Figure 13. Microstructure of untreated AISI 1045 steel at 200× magnification

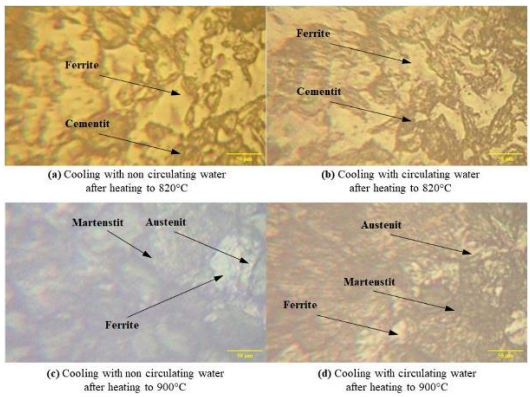

Figure 14. Microstructure of AISI 1045 steel heated at 200× magnification

Figure 14 shows the microstructure of AISI 1045 steel specimens that were heat-treated at 820℃ and quenched in still water. Darker areas are caused by uneven test specimens due to sanding errors. Changes in the microstructure are indicated by the presence of small, needle-like structures, which signify the formation of a martensitic structure. There are still white areas representing the α eutectoid phase that did not fully transform into martensite. The formation of martensite and the α eutectoid phase contribute to the increased hardness of this specimen.

Furthermore, the specimen quenched in running water shows many voids left behind due to imperfect polishing. The amount/volume fraction of martensite appears to be increasing, as indicated by the random arrangement of needle-like shapes. The formation of more martensite structures during quenching in running water, compared to the quenching process without flow (regular immersion), results in the specimen quenched in running water becoming harder, thereby increasing its tensile strength and stress.

The microstructure of the AISI 1045 steel specimen heated at 900℃ and quenched with flowing water shows a fairly even dark area, with no visible grain boundaries. The white circles are no longer clearly visible, as they are in the material quenched without flow. What is clearly visible is the martensitic microstructure, characterized by randomly arranged needle-like shapes. The formation of the martensitic structure causes the specimen quenched with flow to be harder compared to the material quenched without flow. The amount of martensite phase due to rapid cooling significantly affects the mechanical strength of the steel, as martensite generally possesses a non-cubic structure. The trapping of carbon within the lattice further contributes to its strength, making it difficult to slip.

3.5 Practical implications

The incorporation of flowing water cooling in the quenching process of AISI 1045 steel significantly enhances its mechanical properties and microstructural uniformity. In industrial applications, this method can be utilized to produce high-strength, wear-resistant components that meet the stringent demands of sectors such as automotive, construction, and manufacturing [33]. For example, components like axles, gears, and connecting rods, which require a precise balance of strength and toughness, can benefit from the enhanced martensitic transformation achieved through flowing water cooling [34]. The findings indicate that using a controlled flow rate during cooling not only optimizes the tensile strength and

hardness of the steel but also minimizes the likelihood of defects such as microstructural inconsistencies and residual stresses, thereby improving the reliability and lifespan of industrial components [35].

From a process optimization perspective, the adoption of flowing water cooling offers several advantages. This method provides a more controlled and uniform cooling rate compared to static water or other cooling media, resulting in more predictable and consistent material properties [36]. This can lead to reduced material waste and lower rejection rates during quality control. Additionally, the ability to enhance mechanical properties at relatively lower cooling temperatures, as highlighted in this study, translates into energy savings and reduced operational costs. By integrating efficient water recirculation systems and temperature control mechanisms, industries can further minimize environmental impacts while maintaining high productivity and cost-effectiveness [35]. These practical benefits position flowing water cooling as a valuable and sustainable innovation for heat treatment processes in modern manufacturing.

3.6 Environmental impact

The use of flowing water in the quenching process of AISI 1045 steel has significant environmental implications, both positive and challenging. On the positive side, water is an abundant and environmentally friendly cooling medium compared to oil or synthetic solutions, which can pose risks of chemical contamination and hazardous waste [37]. The ability of flowing water to enhance cooling rates and improve material properties also enables energy-efficient processes, as it allows for lower heat treatment temperatures and shorter processing times. This energy efficiency can reduce the overall carbon emissions associated with steel manufacturing, aligning with the industry's sustainability goals [38].

However, the environmental benefits of using flowing water depend on proper system management. High water consumption during continuous flow cooling can strain local water resources if not effectively recycled. Additionally, the discharge of hot water, if untreated, can lead to thermal pollution and negatively impact aquatic ecosystems. To address these challenges, industries must adopt closed-loop cooling systems that recycle water and incorporate heat recovery mechanisms [39]. Proper water treatment before discharge can also ensure compliance with environmental regulations and minimize ecological impacts, making flowing water cooling a more sustainable choice for industrial applications.

4. CONCLUSIONS

The optimal mechanical strength of AISI 1045 steel was achieved at 820°C, yielding a 20.16% enhancement with flowing water-cooling compared to still water. The tensile strength associated with Q_0 has been noted as 67.02 kgf/mm²; conversely, Q_1 is recorded at 92.66 kgf/mm², and Q_2 shows a measurement of 97.83 kgf/mm². Hardness values improved with the quenching process using flowing water, with Q_0 at 13.7 HRC, Q_1 at 32.0 HRC, and Q_2 at 35.8 HRC. The microstructural analysis revealed a more uniform and abundant martensite in specimen Q_2, which underwent flowing water quenching, relative to specimen Q_1 quenched in still water. The cooling rate in water-assisted quenching surpasses that of static water quenching.

ACKNOWLEDGMENT

We express our gratitude to the Head of the Department of Mechanical Engineering at Cenderawasih University for the provision of resources and facilities essential for our experimental research.

REFERENCES

[1] Nasution, M. (2023). Effect of quenching media on the strength of AISI 1045 steel applied to chain sprockets: Impact test method. International Journal of Research and Review, 10(2): 211-215. https://doi.org/10.52403/ijrr.20230227

[2] Padzi, M.M., Abdullah, S., Nuawi, Mohd.Z. (2013). Fatigue damage assessment correlating with I-Kaz coefficient. Applied Mechanics and Materials, 471: 235-240. https://doi.org/10.4028/www.scientific.net/amm.471.235

[3] Zhang, Y., Han, T., Xiao, M., Shen, Y. (2020). Microstructure and properties of laser-clad FeNiCoCrTi0.5Nb0.5 high-entropy alloy coating. Materials Science and Technology, 36(7): 811-818. https://doi.org/10.1080/02670836.2020.1743924

[4] Adam, A.A., Bakar, H.A., Amani, U.A., Paijan, L.H., et al. (2022). Effect of sintering parameters on the mechanical properties and wear performance of alumina inserts. Lubricants, 10(12): 325. https://doi.org/10.3390/lubricants10120325

[5] Ibrahim, A., Sayuti, M. (2015). Effect of heat treatment on hardness and microstructures of AISI 1045. Advanced Materials Research, 1119: 575-579. https://doi.org/10.4028/www.scientific.net/amr.1119.575

[6] Rodríguez-Castro, G.A., Campos-Silva, I., Martínez-Trinidad, J.F., Figueroa-López, U., Meléndez-Morales, D., Vargas-Hernández, J.J. (2009). Effect of boriding on the mechanical properties of AISI 1045 steel. Advanced Materials Research, 65: 63-68. https://doi.org/10.4028/www.scientific.net/amr.65.63

[7] Wenish, G.D., Prince, M., Maniraj, J. (2022). Characterization of induction hardened and tempered AISI 1045 steel. Matéria (Rio de Janeiro), 27: e20220170. https://doi.org/10.1590/1517-7076-rmat-2022-0170

[8] Gao, K., Qin, X., Wang, Z., Chen, H., Zhu, S., Liu, Y., Song, Y. (2014). Numerical and experimental analysis of 3D spot induction hardening of AISI 1045 steel. Journal of Materials Processing Technology, 214(11): 2425-2433. https://doi.org/10.1016/j.jmatprotec.2014.05.010

[9] Martínez-Vázquez, J.M., Rodríguez-Ortiz, G., Hortelano-Capetillo, J.G., Pérez-Pérez, A. (2021). Effect of induction heating on Vickers and Knoop hardness of 1045 steel heat treated. Journal of Mechanical Engineering, 5(15): 8-15. https://doi.org/10.35429/jme.2021.15.5.8.15

[10] Mishra, A., Saha, A., Maity, J. (2015). Microstructure evolution in AISI 1080 eutectoid steel under cyclic quenching treatment. Metallography, Microstructure,

and Analysis, 4(5): 355-370. https://doi.org/10.1007/s13632-015-0222-4
[11] Pereloma, E., Edmonds, D.V. (2012). Phase Transformations in Steels. Oxford (GB): Woodhead Publishing.
[12] Vieira, E.d.R., Biehl, L.V., Medeiros, J.L.B., Costa, V.M., Macedo, R.J. (2021). Evaluation of the characteristics of an AISI 1045 steel quenched in different concentration of polymer solutions of polyvinylpyrrolidone. Scientific Reports, 11(1): 1313. https://doi.org/10.1038/s41598-020-79060-0
[13] Kadowaki, M., Muto, I., Sugawara, Y., Doi, T., Kawano, K., Hara, N. (2017). Pitting corrosion resistance of martensite of AISI 1045 steel and the beneficial role of interstitial carbon. Journal of the Electrochemical Society, 164(14): C962-C972. https://doi.org/10.1149/2.0541714jes
[14] Nishimoto, M., Muto, I., Doi, T., Kawano, K., Sugawara, Y. (2022). Effect of quenching in aqueous polyvinylpyrrolidone solutions on the microstructure and pitting corrosion resistance of AISI 1045 carbon steel. Materials and Corrosion, 74(5): 724-733. https://doi.org/10.1002/maco.202213658
[15] Nekouei, R.K., Akhaghi, R., Ravanbakhsh, A., Tahmasebi, R., Moghaddam, A.J., Mahrouei, M. (2016). A study of the effect of two-stage tempering on mechanical properties of steel 30CrMnSi using analysis on response surface in design of experiment. Metal Science and Heat Treatment, 57(11-12): 694-701. https://doi.org/10.1007/s11041-016-9945-3
[16] Al-Kabi, S.H.A., Al-Ghzawi, B.A.H.K., Ahmed, I.H., Al-Mutoki, S.M.M., Al-Kaneyni, H. (2023). The effect of quenching in different concentrations of alumina nano fluids on overall properties of Al-6061. Annales de Chimie - Science des Matériaux, 47(2): 105-110. https://doi.org/10.18280/acsm.470207
[17] Callister, W.D. (2007). Materials Science and Engineering: An Introduction (7th ed.). New York: John Wiley & Sons.
[18] Smith, W.F., Hashemi, J., Presuel-Moreno, F. (2019). Foundations of Materials Science and Engineering (Sixth edition.). New York, NY: McGraw-Hill Education.
[19] Farber, V.M., Selivanova, O.V., Arabey, A.B., Polukhina, O.N., Mamatnazarov, A.S. (2014). Effect of heat treatment on mechanical properties of steels of strength class K65 (X80). Metal Science and Heat Treatment, 56(7-8): 454-456. https://doi.org/10.1007/s11041-014-9781-2
[20] Van Bohemen, S.M.C., Sietsma, J. (2008). Modeling of isothermal bainite formation based on the nucleation kinetics. International Journal of Materials Research, 99(7): 739-747. https://doi.org/10.3139/146.101695
[21] Wang, B., Chen, S., Chen, W. (2015). Effect of quenching and tempering treatment on the microstructure and properties of Q345B casting. In 2015 International Conference on Economy, Management and Education Technology, Tianjin, China, pp. 385-390. https://doi.org/10.2991/icemet-15.2015.83
[22] Huyan, F., Hedström, P., Höglund, L., Borgenstam, A. (2016). A thermodynamic-based model to predict the fraction of martensite in steels. Metallurgical and Materials Transactions A, 47(9): 4404-4410. https://doi.org/10.1007/s11661-016-3604-6
[23] Sista, V., Nash, P., Sahay, S.S. (2007). Accelerated bainitic transformation during cyclic austempering. Journal of Materials Science, 42(21): 9112-9115. https://doi.org/10.1007/s10853-007-2065-0
[24] Liu, Y. (2002). Influence of plasticity on transformation behaviour of martensite in NiTi. In IUTAM Symposium on Mechanics of Martensitic Phase Transformation in Solids: Proceedings of the IUTAM Symposium, Hong Kong, China, pp. 155-162. https://doi.org/10.1007/978-94-017-0069-6_19
[25] Iqbal, S.A., Mativenga, P.T., Sheikh, M.A. (2007). Characterization of machining of AISI 1045 steel over a wide range of cutting speeds. Part 2: Evaluation of flow stress models and interface friction distribution schemes. Proceedings of the Institution of Mechanical Engineers, Part B: Journal of Engineering Manufacture, 221(5): 917-926. https://doi.org/10.1243/09544054JEM797
[26] Mattavelli, D., Cislaghi, L., Rosso, M., Ugues, D. (2008). Austempering effect on structure properties and performances of hot-work tool steel. International Journal of Microstructure and Materials Properties, 3(2/3): 216-230. https://doi.org/10.1504/IJMMP.2008.018729
[27] Haitao, J., Miaoquan, L. (2004). Effects of isothermal heat treatment on microstructural evolution of semisolid Al-4Cu-Mg alloy. Journal of Materials Engineering and Performance, 13(4): 488-492. https://doi.org/10.1361/10599490420034
[28] Liang, X., DeArdo, A.J. (2014). A study of the influence of thermomechanical controlled processing on the microstructure of bainite in high strength plate steel. Metallurgical and Materials Transactions A, 45(11): 5173-5184. https://doi.org/10.1007/s11661-014-2444-5
[29] Odusote, J.K., Ajiboye, T.K., Rabiu, A.B. (2012). Evaluation of mechanical properties of medium carbon steel quenched in water and oil. Journal of Minerals and Materials Characterization and Engineering, 11: 859-862. https://doi.org/10.4236/jmmce.2012.119079
[30] Putri, F., Gunawan, I., Rizky, D.A. (2023). The effect of quenching treatment by variation of cooling media (water, used oil, cooking oil) on EGREK hardness. AUSTENIT, 15(1): 13-20. https://doi.org/10.53893/austenit.v15i1.5450
[31] Haissam, A., Benarrache, S., Rahmani, R.K., Mansouri, T., Benhorma, M.E. (2024). Effect of heat treatments on the mechanical and microstructure properties of welded API X70 steel. Annales de Chimie - Science des Matériaux, 48(4): 551-557. https://doi.org/10.18280/acsm.480412
[32] Giordani, T., Clarke, T., Kwietniewski, C.E.F., Aronov, M.A., Kobasko, N.I., Totten, G.E. (2013). Mechanical and metallurgical evaluation of carburized, conventionally and intensively quenched steels. Journal of Materials Engineering and Performance, 22(8): 2304-2313. https://doi.org/10.1007/s11665-013-0522-2
[33] Iakovakis, E., Avcu, E., Roy, M.J., Gee, M., Matthews, A. (2022). Wear resistance of an additively manufactured high-carbon martensitic stainless steel. Scientific Reports, 12(1): 12554. https://doi.org/10.1038/s41598-022-15621-9
[34] Joni, J., Bhiftime, E.I., Ranteallo, O., Dewa, R.T., et al. (2024). Corrosion and microstructure on the casting product propeller shaft model of Al6063 aluminum alloy base materials. Key Engineering Materials, 975: 53-61. https://doi.org/10.4028/p-8wsQ0Q

[35] Klinar, K., Swoboda, T., Muñoz Rojo, M., Kitanovski, A. (2021). Fluidic and mechanical thermal control devices. Advanced Electronic Materials, 7(3): 2000623. https://doi.org/10.1002/aelm.202000623
[36] Pontes, R.F.F., Pinto, J.M., Silva, E.K.G. (2022). Optimal design and operation of cooling water pumping systems. Computers & Chemical Engineering, 157: 107581. https://doi.org/10.1016/j.compchemeng.2021.107581
[37] Vigneshwaran, K., Sodhi, G.S., Muthukumar, P., Guha, A., Senthilmurugan, S. (2019). Experimental and numerical investigations on high temperature cast steel based sensible heat storage system. Applied Energy, 251: 113322. https://doi.org/10.1016/j.apenergy.2019.113322
[38] Adefarati, T., Obikoya, G.D. (2020). Assessment of renewable energy technologies in a standalone microgrid system. International Journal of Engineering Research in Africa, 46: 146-167. https://doi.org/10.4028/www.scientific.net/JERA.46.146
[39] Jun, L., Ma, C., Tao, W., Chang, J., Zhao, X. (2019). Effects of roughness on the performance of axial flow cyclone separators using numerical simulation method. Proceedings of the Institution of Mechanical Engineers, Part A: Journal of Power and Energy, 233(7): 914-927. https://doi.org/10.1177/0957650919831892